

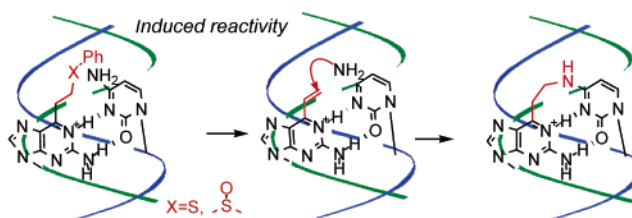
Hybridization-Promoted and Cytidine-Selective Activation for Cross-Linking with the Use of 2-Amino-6-vinylpurine Derivatives

Takeshi Kawasaki,[†] Fumi Nagatsugi,^{†,‡} Md. Monsur Ali,^{†,‡} Minoru Maeda,[†]
Kumiko Sugiyama,[§] Kenji Hori,[§] and Shigeki Sasaki*,^{†,‡}

Graduate School of Pharmaceutical Sciences, Kyushu University, 3-1-1 Maidashi, Higashi-ku, Fukuoka 812-8582, Japan, CREST, Japan Science and Technology Agency, Kawaguchi Center Building, 4-1-8 Honcho, Kawaguchi, Saitama 332-0012, Japan, and Faculty of Engineering, Yamaguchi University, Tokiwadai, Ube 755-8611, Japan

sasaki@phar.kyushu-u.ac.jp

Received September 24, 2004



Recently, we have proposed a new concept for cross-linking agents with inducible reactivity, in which the highly reactive cross-linking agent, the 2-amino-6-vinylpurine nucleoside analogue (**1**), can be regenerated in situ from its stable precursors, the phenylsulfide (**4**) and the phenylsulfoxide (**3**) derivatives, by a hybridization-promoted activation process with selectivity to cytidine. The phenylsulfide precursor (**4**) exhibited cross-linking ability despite its high stability toward strong nucleophiles such as amines and thiols. In this study, we investigated the substituent effects of the phenylsulfide group on the cross-linking reaction, and determined the 2-carboxy substituent of the phenylsulfide derivative (**11k**) as an efficient cross-linking agent with inducible reactivity. Detailed investigations have shown that the phenylsulfoxide (**3**) and phenylsulfide (**4**) precursors produce the 2-amino-6-vinylpurine nucleoside (**1**) as the common reactive species. It has been concluded that the nature of the inducible reactivity of the precursors (**3** and **4**) is acceleration of their elimination to the 2-amino-6-vinylpurine nucleoside (**1**) through the selective process in the duplex with the ODN having cytidine at the target site.

Introduction

Oligodeoxynucleotides (ODN) and their analogues have been widely used for the inhibition of gene expression in antisense or antigene methods, etc.¹ ODNs attaching a functional reagent may cause irreversible change to the target sequence.² Inhibition of the elongation step has been achieved by the use of reactive antisense ODNs conjugating a group for alkylation.^{3–5} Furthermore, site-

directed mutagenesis (or site-directed manipulation of genes) toward the target duplex has been proposed as a new biological tool with the use of a triplex-forming oligonucleotide.^{6,7} Strand invasion has been recently demonstrated by the use of ODNs attaching a cross-linking agent to triplex-forming guide sequences.⁸ Interest in a variety of potential applications of reactive ODNs has encouraged us to generate new cross-linking agents that might be applicable to both in vitro and in vivo studies.

There are several types of alkylating agents that have been conjugated to the ODNs.⁹ Halocarbonyl^{10–16} or

* Address correspondence to this author. Phone: 81-92-642-6615. Fax: 81-92-642-6876.

[†] Kyushu University.

[‡] CREST, Japan Science and Technology Agency.

[§] Yamaguchi University.

(1) A comprehensive review: Murray, J. A., Ed. *Antisense RNA and DNA*; John Wiley & Sons, INC.: New York, 1992.

(2) Beaucage, S. L.; Iyer, R. P. *Tetrahedron* **1993**, *49*, 1295–1963.

(3) Kean, J. M.; Murakami, A.; Blake, K.; Cushman, C.; Miller, P. S. *Biochemistry* **1988**, *27*, 9113–9121.

(4) Lee, B. L.; Murakami, A.; Blake, K. R.; Lin, S.-B.; Miller, P. S. *Biochemistry* **1988**, *27*, 3197–3203.

(5) Boiziau, C.; Kurfurst, R.; Caceneve, C.; Roig, V.; Thuong, N. T.; Toulme, J.-J. *Nucleic Acids Res.* **1991**, *19*, 1113–1119.

(6) Woolf, T. M. *Nature Biotechnol.* **1988**, *16*, 341–344.

(7) Chan, P. P.; Lin, M.; Faruqi, A. F.; Powell, J.; Seidman, M. M.; Glazer, P. M. *J. Biol. Chem.* **1999**, *274*, 11541–11548.

(8) Gamper, H. B., Jr.; Hou, Ya-M.; Stamm, M. R.; Podyminogin, M. A.; Meyer, R. B. *J. Am. Chem. Soc.* **1998**, *120*, 2182–2183.

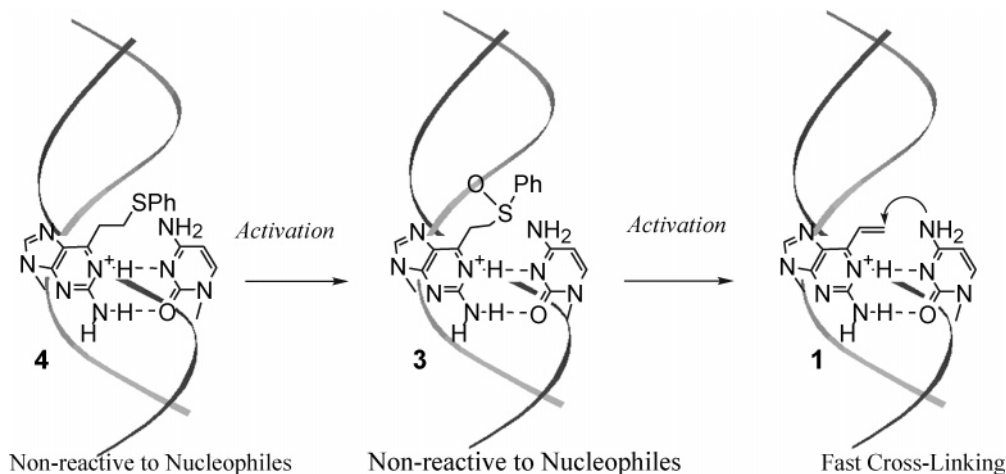
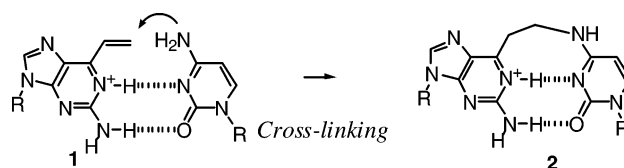


FIGURE 1. The new concept of cross-linking agent that can be activated in situ by duplex formation as the trigger.

aziridine^{17–20} groups alkylated bases in an S_N2 manner (S_N2 reagents). Highly reactive functional groups such as haloacetyl have been used for alkylation at N7 of guanosine, whereas their high reactivities might suffer disadvantages for biological applications. As the alkylating group of ODNs should receive nucleophilic attack by a number of chemical entities in the living system such as water, amines, and thiols, etc., achievement of both high reactivity and stability of the alkylating group falls into a dilemma. A promising approach to overcome such problems is the use of agents that have inducible reactivity by triggering signals such as UV-irradiation, enzymatic, or chemical reactions. Some compounds, such as ET-743 and CC-1065, are furnished with inducible reactivity that is activated in the microenvironments of the DNA.^{21–26} Psoralen and its analogues have enjoyed remarkable successes as T-selective photo-cross-linking agents that are applied to a wide variety of in vitro as

SCHEME 1. Selective Cross-Linking of Cytosine by 2-Amino-6-vinylpurine (1)



well as in vivo studies.^{27–31} However, as UV irradiation might cause damages to other sites of DNA and UV light might not be suitable for in vivo study, researchers have been seeking other types of alkylating agents with inducible reactivity. Rokita's group developed the intermediates of a quinone methide as inducible alkylating agents that can be activated by enzymatic reduction^{32,33} or chemical reaction.^{34–36} Quinone methide derivatives have been used to propose a general strategy for target-promoted alkylation.³⁷ An interesting cross-linking reaction has been proposed in the hybridization-activated conversion of the manondialdehyde M1G adduct to ring-opened oxopropenyl-dG adduct.³⁸

Our group has developed 2-amino-6-vinylpurine nucleoside (1) as a selective cross-linking agent to cytosine (Scheme 1).^{39,40} In our original design, a close proximity

(9) A recent review: Sasaki, S. *Eur. J. Pharm. Sci.* **2001**, *13*, 43–51.

(10) Coleman, R. S.; Pires, R. M. *Nucleic Acids Res.* **1997**, *25*, 4771–4777.

(11) Coleman, R. S.; Kesicki, E. A. *J. Org. Chem.* **1995**, *60*, 6252–6253.

(12) Tabone, J. C.; Stamm, M. R.; Gamper, H. B.; Meyer, R. B., Jr. *Biochemistry* **1994**, *33*, 375–383.

(13) Meyer, R. B., Jr.; Tabone, J. C.; Hurst, G. D.; Smith, T. M.; Gamper, H. *J. Am. Chem. Soc.* **1989**, *111*, 8517–8519.

(14) Grant, K. B.; Dervan, P. B. *Biochemistry* **1996**, *35*, 12313–12319.

(15) Povsic, T. J.; Strobel, S. A.; Dervan, P. B. *J. Am. Chem. Soc.* **1992**, *114*, 5934–5941.

(16) Povsic, T. J.; Dervan, P. B. *J. Am. Chem. Soc.* **1990**, *112*, 9428–9430.

(17) Webb, T. R.; Matteucci, M. D. *J. Am. Chem. Soc.* **1986**, *108*, 2764–2765.

(18) Webb, T. R.; Matteucci, M. D. *Nucleic Acids Res.* **1986**, *14*, 7661–7674.

(19) Cowart, M.; Benkovic, S. J. *Biochemistry* **1991**, *30*, 788–796.

(20) Shaw, J.-P.; Milligan, J. F.; Krawczyk, S. H.; Matteucci, M. D. *J. Am. Chem. Soc.* **1991**, *113*, 7765–7766.

(21) Zewail-Foote, M.; Hurley, M. H. *J. Med. Chem.* **1999**, *42*, 2493–2497.

(22) Afonina, I.; Zivarts, M.; Kutyavin, I. V.; Lukhtanov, E. A.; Gamper, H.; Meyer, R. B. *J. Am. Chem. Soc.* **1997**, *119*, 6214–6225.

(23) Lukhtanov, E. A.; Podyminogin, M. A.; Kutyavin, I. V.; Meyer, R. B.; Gamper, H. B. *Nucleic Acids Res.* **1996**, *24*, 683–687.

(24) Dempcy, R. O.; Kutyavin, I. V.; Mills, A. G.; Lukhtanov, E. A.; Meyer, R. B. *Nucleic Acids Res.* **1999**, *27*, 2931–2937.

(25) Reed, M. W.; Wald, A.; Meyer, R. B. *J. Am. Chem. Soc.* **1998**, *120*, 9729–9734.

(26) Lukhtanov, E. A.; Mills, A. G.; Kutyavin, I. V.; Gorn, V. V.; Reed, M. W.; Meyer, R. B. *Nucleic Acids Res.* **1997**, *25*, 5077–5084

(27) Murakami A.; Yamayoshi, A.; Iwase, R.; Nishida, J.; Yamaoka, T.; Wake, N. *Eur. J. Pharm. Sci.* **2001**, *13*, 25–34.

(28) Takasugi, M.; Guendouz, A.; Chassignon, M.; Decout, J. L.; Lhomme, J.; Thuong, N. T.; Helene, C. *Proc. Natl. Acad. Sci. U.S.A.* **1991**, *88*, 5602–5606.

(29) Puri, N.; Majumdar, A.; Cuenoud, B.; Natt, F.; Martin, P.; Boyd, A.; Miller, P. S.; Seidman, M. M. *J. Biol. Chem.* **2001**, *276*, 28991–28998.

(30) Musso, M.; Wang, J. C.; Vandyke, M. W. *Nucleic Acids Res.* **1996**, *24*, 492–493.

(31) Grigoriev, M.; Praseuth, D.; Guieysse, A. L.; Robin, P.; Thuong, N. T.; Helene, C.; Bellan-H. A. *Proc. Natl. Acad. Sci. U.S.A.* **1993**, *90*, 3501–3505

(32) Chatterjee, M.; Rokita, S. E. *J. Am. Chem. Soc.* **1994**, *116*, 1690–1697.

(33) Chatterjee, M.; Rokita, S. E. *J. Am. Chem. Soc.* **1991**, *113*, 5116–5117.

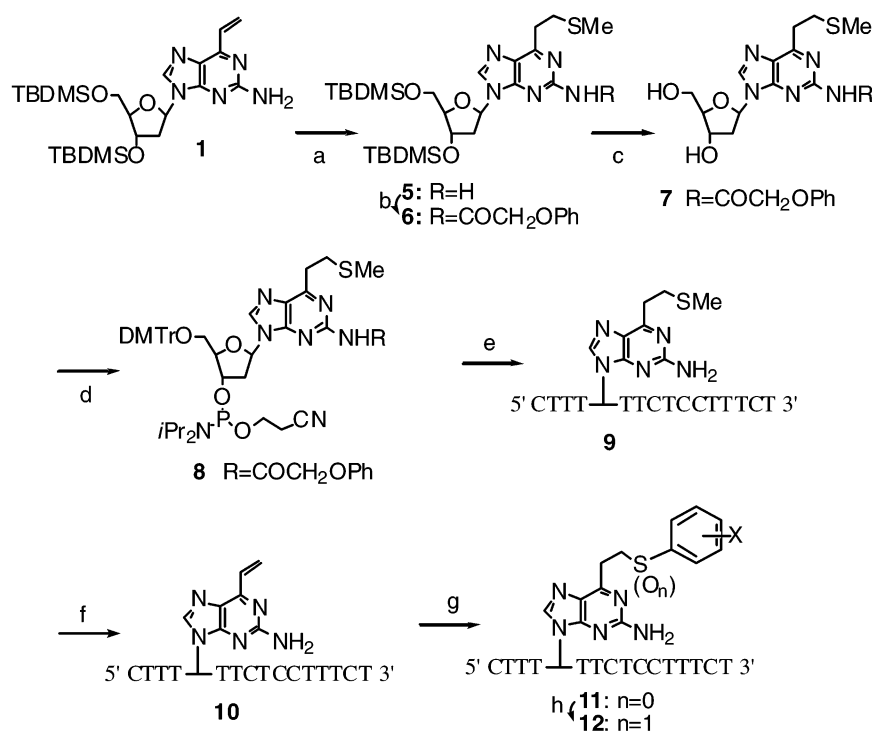
(34) Pande, P.; Shearer, J.; Yang, J.; Greenberg, G. A.; Rokita, S. E. *J. Am. Chem. Soc.* **1999**, *121*, 6775–6779.

(35) Zeng, Q.; Rokita, S. E. *J. Org. Chem.* **1996**, *61*, 9080–9081.

(36) Li, T.; Zeng, Q.; Rokita, S. E. *Bioconj. Chem.* **1994**, *5*, 497–500.

(37) Zhou, Q. B.; Rokita, S. E. *Proc. Natl. Acad. Sci. U.S.A.* **2003**, *100*, 15452–15457.

(38) Mao, H.; Schnetz-Boutaud, N. C.; Weisenseel, J. P.; Marnett, L. J.; Stone, M. P. *Proc. Natl. Acad. Sci. U.S.A.* **1999**, *96*, 6615–6620.

SCHEME 2. The Synthesis of the Oligodeoxynucleotides Incorporating the Cross-Linking Agent^a

^a Reagents and conditions: (a) MeSNa, CH₃CN, (b) PhOCH₂COCl, 1-HBT, pyridine, CH₃CN, (c) TBAF, THF, (d) (1) DMTrCl, pyridine, (2) *i*Pr₂NP(Cl)OC₂H₄CN, *i*Pr₂NEt, CH₂Cl₂, (e) (1) automated DNA synthesizer, (2) 0.1 N NaOH, (3) neutralized AcOH, (4) 10% AcOH, (f) (1) 3.0 equiv of MMPP, pH 10, (2) 470 mM NaOH, (g) X-PhSH, (h) 3.0 equiv of MMPP, pH 10.

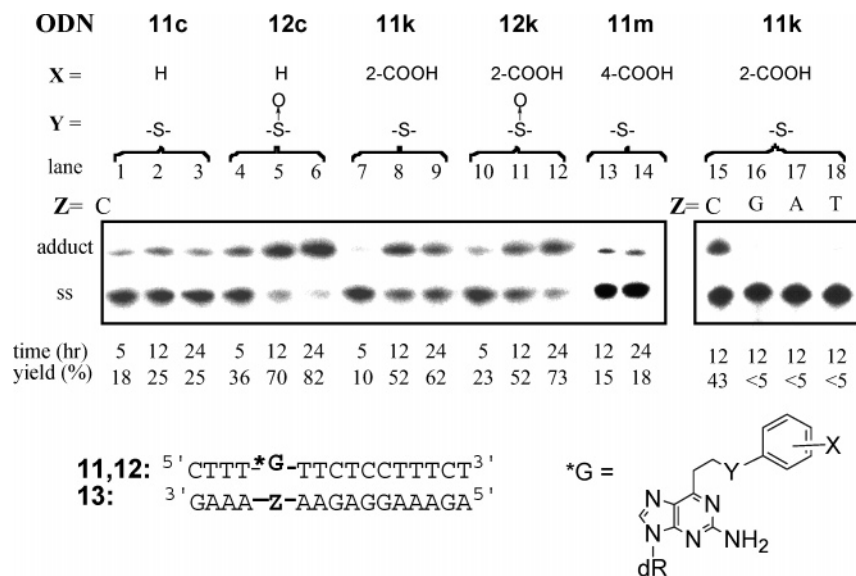


FIGURE 2. Gel electrophoresis of the cross-linking reaction. The reaction was performed with 7 μM ODNs (**11** or **12**) and 3 μM target ODN (**13**) including a labeled one with ³²P at the 5' end as a tracer in 0.1 M NaCl, 50 mM MES, pH 5.0, 30 $^{\circ}\text{C}$.

of the 4-amino group of cytidine to the vinyl group of **1** was expected in the complex between the protonated form of **1** and cytidine to work effectively for covalent bond formation.³⁹

The structure of this alkylating agent is unique in that both the reactive site and the recognition site are built

in a single molecule. Furthermore, the reactivity of the vinyl group could be adjusted by substitution on the vinyl group with an electron-donating group for slower rate⁴⁰ or an electron-withdrawing group for faster rate under neutral conditions.⁴¹ In a new application, site-directed mutagenesis has been achieved by the use of the triplex-forming oligonucleotides incorporating the 2-amino-6-

(39) Nagatsugi, F.; Uemura, K.; Nakashima, S.; Maeda, M.; Sasaki, S. *Tetrahedron Lett.* **1995**, *36*, 421–424.

(40) Nagatsugi, F.; Uemura, K.; Nakashima, S.; Maeda, M.; Sasaki, S. *Tetrahedron* **1997**, *53*, 3035–3044.

(41) Nagatsugi, F.; Tokuda, N.; Maeda, M.; Sasaki, S. *Bioorg. Med. Chem. Lett.* **2001**, *11*, 2577–2579.

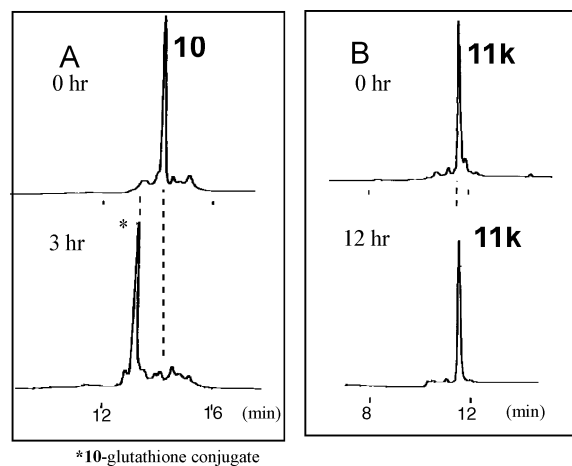


FIGURE 3. Analysis of the reaction of **10** (A) and **11k** (B) with 1 mM Glutathione. A mixture of 10 μ M ODN and 1 mM glutathione was kept at 37 $^{\circ}$ C in the buffer containing 0.1 M NaCl, 10 mM KH_2PO_4 , pH 5.0. HPLC conditions: ODS column, 1.0 mL/min; solvent A = 0.1 M TEAA; solvent B = CH_3CN , linear gradient from 10% to 30% over 20 min, 30% to 100% over 30 min, monitored at 254 nm.

vinylpurine derivative.⁴² While studying new cross-linking agents, we proposed a new strategy of inducible reactivity, in which a reactive species is generated in situ from its stable precursors in close proximity with a target base in the duplex. The validity of this concept has been successfully demonstrated in the previous study by the fact that the phenylsulfoxide (**3**) is activated in situ by

TABLE 1. Substituent Effect on the Cross-Linking Reaction^a

compd	X	yield (%)	
		11 (sulfide)	12 (sulfoxide) ^b
a	4-NO ₂	9	66
b	4-Br	14	56
c	4-H	25	82
d	4-OMe	30	81
e	4-OH	30	78
f	4-Me	37	83
g	4-NH ₂	44	—
h	2,4-Me ₂	28	—
i	3,4-(MeO) ₂	37	—
j	2,4,6-Me ₃	42	—
k	2-COOH	62	73
m	4-COOH	18	—

^a Yield was determined by gel electrophoresis at 24 h. Reaction was performed as described in the footnote of Figure 2. ^b The reaction was not performed in the column marked with “—”.

hybridization with a complementary strand to produce efficient and selective cross-linking to cytidine (Figure 1).⁴³ An interesting finding from a practical viewpoint was that the phenylsulfide precursor (**4**) produced cross-linked products despite its high stability toward strong nucleophiles such as amines and thiols. The ODN having the phenylsulfide precursor (**4**) are currently under evaluation for antisense effects in biological studies. In this study, we investigated the substituent effects of the phenylsulfide group on the cross-linking reaction, and determined the 2-amino-6-[2-(2-carboxyphenylthio)ethyl]-purine precursor (**11k**) as an efficient cross-linking agent

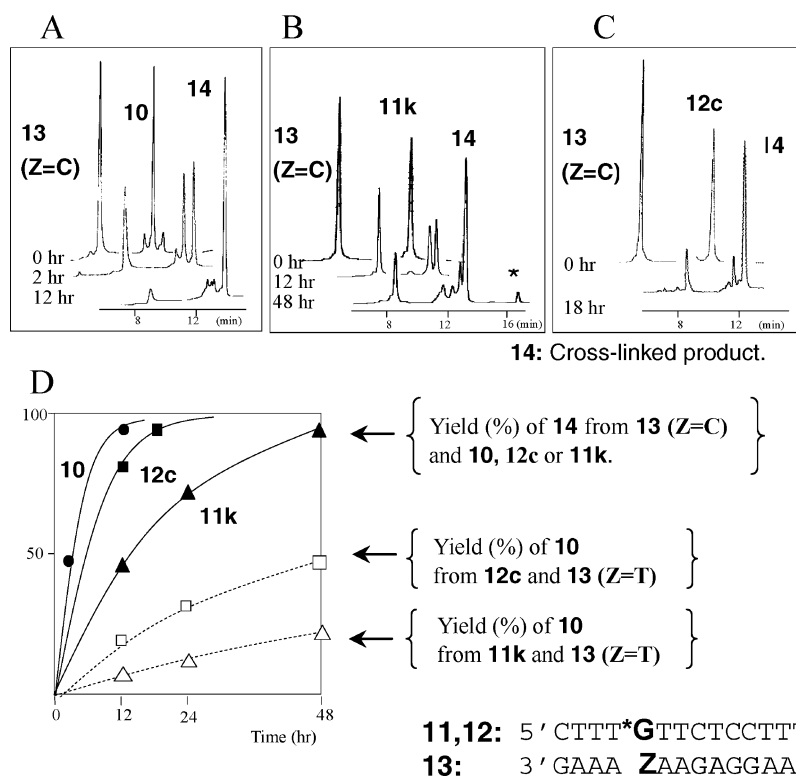


FIGURE 4. HPLC analysis of the cross-linking reaction with **10** (A), **11k** (B), and **12c** (C) and comparison of the reaction yield (D). The peak labeled with **14** corresponds to the cross-linked product. A 0.3 mM sample of each oligomer was used in 300 μ L of H_2O buffer containing 0.1 M NaCl and 50 mM MES at pH 5.0. HPLC conditions: ODS column, 1.0 mL/min; solvent A = 0.1 M TEAA; solvent B = CH_3CN , linear gradient from 0% to 30% over 20 min, 30% to 100% over 30 min, monitored at 254 nm. The peak marked with an asterisk (*) in B indicates 2-carboxyphenyl disulfide.



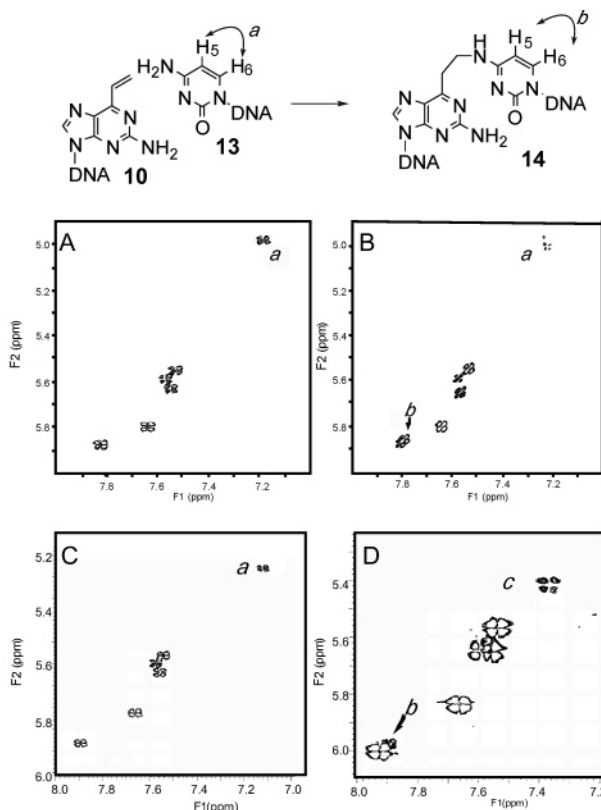
with inducible reactivity. Here we wish to describe a detailed study on the mechanism of the inducible reactivity of the phenylsulfide (**4**) and phenylsulfoxide precursors (**3**) to prove that they produce the 2-amino-6-vinylpurine nucleoside analogue (**1**) as the common reactive species, and that the nature of their inducible reactivity is selective acceleration of their elimination to the vinyl structure in the duplex having cytidine at the target site.

Results

Synthesis of ODNs Incorporating 2-Amino-6-vinylpurine Derivatives. We have previously used the phenylsulfide (–SPh) derivative of the 2-amino-6-vinylpurine nucleoside (**1**) for incorporation into the ODNs.⁴³ However, it turned out that the phenylsulfide group was not suitable for the synthesis of some DNA sequences such as G-rich ones. Therefore, we utilized the methylsulfide (–SMe) group as a more stable protecting group of the vinyl group of **1** in this study. The synthesis of the ODN incorporating the 2-amino-6-vinylpurine derivatives (**9–12**) is summarized in Scheme 2. The 2'-deoxynucleoside derivative of 2-amino-6-vinylpurine (**1**) was synthesized from 2'-deoxyguanosine as described previously.⁴⁰ Treatment of **1** with sodium methanesulfide (MeSNa) in CH₃CN gave a 6-(2-ethylthiomethyl)purine derivative (**5**), followed by protection of the 2-amino group with a phenoxyacetyl group (–COCH₂Oph) and subsequent deprotection of the TBDMS group with *n*-tetrabutylammoniumfluoride (TBAF) to afford the diol product (**7**). The amidite precursor (**8**) was synthesized by a standard procedure with 2-cyanoethyl-*N,N*-diisopropylchlorophosphoramidite and applied to an automated DNA synthesizer. Synthesized ODN was cleaved from the solid support with 0.1 M NaOH solution and purified by HPLC. The terminal 5'-dimethoxytrityl group was deprotected with 10% acetic acid to give ODN (**9**), which was further purified by HPLC. The subsequent treatment with MMPP and aqueous NaOH solution produced **10** having a vinyl motif. To search for the proper phenylsulfide structure for in situ activation, we synthesized a series of substituted phenylsulfide derivatives (**11**) by the addition of the corresponding thiophenol derivatives to **10**. Some of the phenylsulfide compounds were oxidized with MMPP to give **12**. Structures of the substituent groups are shown in Table 1.

Cross-Linking Study with Substituted Phenylsulfide Derivatives. The cross-linking reaction was investigated by using the reactive ODNs (**10**, **11**, and **12**) and the complementary strand (**13**). Reactions were performed for 24 h at 30 °C with 7.0 μM of the reactive ODNs and 3.0 μM of the target strand (**13**) containing the 5'-³²P-labeled target strand as a tracer at pH 5.0, and were analyzed by gel electrophoresis with denatured polyacrylamide gel, and some representative examples are shown in Figure 2.

The cross-linked product was identified as the less mobile bands, and the cross-linking yields were obtained by quantification of the radioactivity of each band; the



10: 5' CTTT*G-TTCTCCTTTCT³' **10:** *G=2-amino-6-vinylpurine,
13: 3' GAAA-C-AAGAGGAAAGA 5' **15:** *G=G

FIGURE 5. 2D-DQF COSY spectra of the duplexes: (A) reaction mixture at 0 h and (B) at 18 h; (C) natural duplex **15** with **13**; (D) isolated **14**. A 1.3 mM sample of each oligomer was reacted in 300 μL of D₂O buffer containing 0.1 M NaCl and 5 mM KH₂PO₄ at pH 5.0. Spectrum D was taken at pH 7.0. The 2D-DQF COSY spectra were recorded at 600 MHz at 30 °C with sweep widths of 6500 Hz in both dimension. The residual HDO peak was suppressed by presaturation. The DQF-COSY spectrum consisted of 2048 datapoints in *t*₂ and 256 increments in *t*₁.

yields at 24 h are summarized in Table 1. Regardless of the substituent X of the phenyl ring, the sulfoxide precursors (**12**) produced the efficient cross-linking reaction. On the other hand, substituent effects were clearly observed in the reaction with the sulfide precursors (**11**). Introduction of the electron-withdrawing group on the phenyl ring decreased the yield (**11a** and **11b** vs **11c**), whereas the yield was increased with the electron-donating group (**11d–j** vs **11c**). Interestingly, **11k** (X = 2-COOH) exhibited the highest yield (62% yield). High selectivity of **11k** to cytidine was clearly observed (Figure 2, lanes 15–18). It is also apparently shown that the ortho position of carboxylic acid of **11k** is important for the efficient reaction, because para-substituted sulfide derivative (**11m**) gave only low yield. Under the conditions where **10** produced the conjugate adduct with glutathione in excellent yield, **11k** exhibited high stability (Figure 3B). As **11k** gradually produces **10** under acidic conditions as explained later (Figure 4D), the results of Figure 3B imply that such transformation is inhibited by glutathione.

Comparison of the Reaction Rates. The cross-linking reaction was also followed by HPLC analysis, and

(42) Nagatsugi, F.; Sasaki, S.; Miller, P. S.; Seidman, M. M. *Nucleic Acids Res.* **2003**, *31*, e31.

(43) Nagatsugi, F.; Kawasaki, T.; Usui, D.; Maeda, M.; Sasaki, S. *J. Am. Chem. Soc.* **1999**, *121*, 6753–6754.

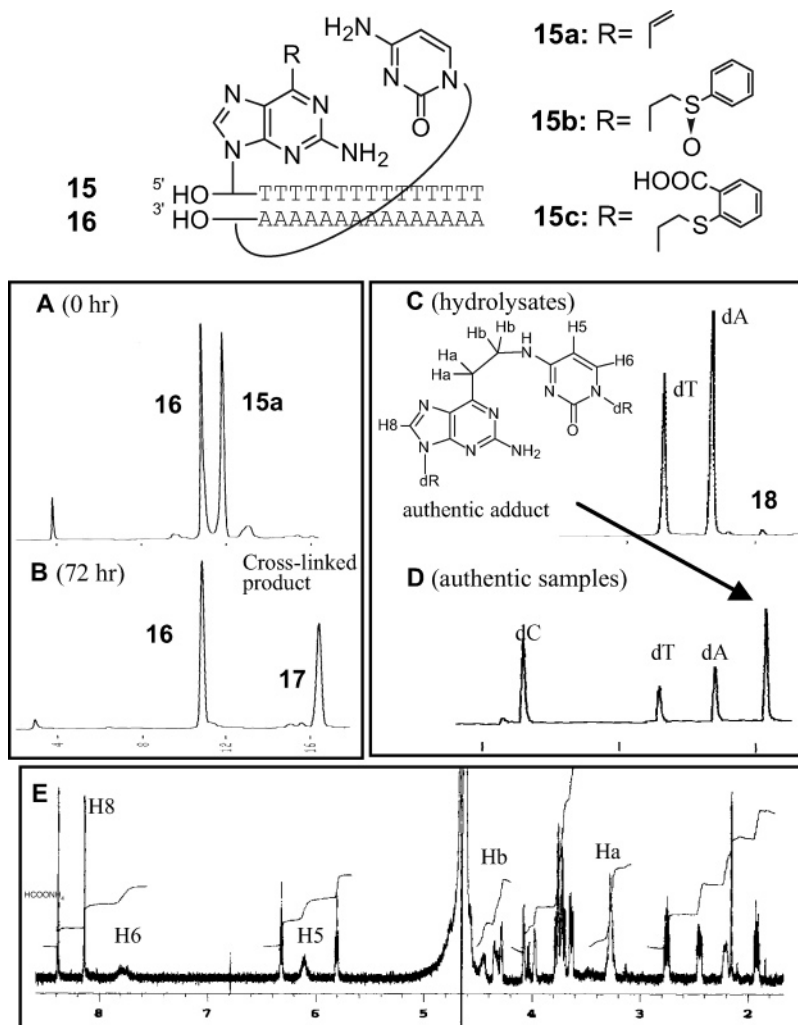


FIGURE 6. HPLC analysis of the cross-linking reaction between **16** and **15a** (A and B), and the adducts from the enzymatic hydrolysate (C and D). For parts A and B the cross-linking reaction conditions are the same as the footnote to Figure 5, and the HPLC conditions are the same as the footnote to Figure 3. The peak **17** was isolated and digested with snake venom phosphodiesterase I (0.6 u/ μ L) and bacterial alkaline phosphatase (0.4 u/ μ L) in 1 μ L of buffer (50 mM Tris-HCl, 5 mM MgCl₂). HPLC conditions for parts C and D: ODS column, 1 mL/min; solvent A = 50 mM ammonium formate, solvent B = CH₃CN, linear gradient from 5% to 30% over 20 min, 30% to 100% over 30 min, monitored at 254 nm. (E) NMR spectra of the adducts obtained from the enzymatic hydrolyzate.

the chromatogram changes are summarized in Figure 4. The reaction was performed at 30 °C in the buffer containing 0.1 M NaCl and 50 mM MES at pH 5.0 by using 0.3 mM each ODNs (**10**, **11k**, and **12c**) and the target ODN (**13**) with cytidine at the reaction site. The peaks corresponding to **14** in Figure 4, panels A, B, and C, were isolated, and proven to be the cross-linked adducts by MALDI-TOF MS measurements. These adducts showed the identical ¹H NMR spectra as described below. Three reactive ODNs exhibited efficient cross-linking with the reaction rate in the order of **10**, **12c**, and **11k** (Figure 4D). We reported previously that the reaction with the ODN (**10**) at micromolar concentrations gave only moderate yield (<50%).⁴³ We observed that decomposition of **10** competed with the cross-linking reaction under low concentrations. In contrast, almost no decomposition of **10** was detected at the high concentrations, probably because the vinyl group of **10** is protected in the duplex. Thus, instability of the vinyl

group of **10** may account for the lower yield at low concentrations.

It was observed by HPLC and MALDI-TOF MS that **10** was formed in the reaction mixture of the phenylsulfide-ODN (**11k**) or the phenylsulfonamide-ODN (**12c**) with the nontarget ODN (**13**: Z = T), clearly showing that **10** is the active intermediate in the cross-linking with **11k** and **12c**. The single strands of **11k** and **12c** are quite stable under neutral conditions, but slowly form **10** together with unknown decomposed materials under the acidic conditions used for the cross-linking reactions. These formation rates of **10** are slower than those observed within the nontarget double strand (Z = T), showing that the reactivity of the cross-linking agents is selectively induced in the duplex having cytidine at the target site. Such sequence-selective activation mechanisms also must be responsible for high selectivity to cytidine (Figure 2). In the reaction with **11k**, 2-carboxyphenyl disulfide was released (the peak marked with an

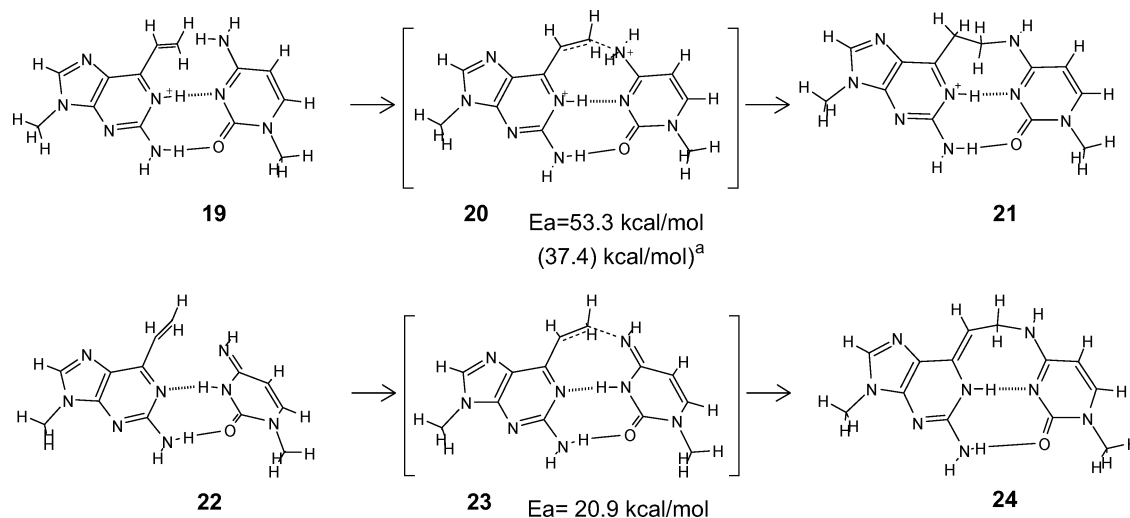


FIGURE 7. Calculated pathway of cross-linking with the 2-amino-6-vinylpurine (**1**) and estimated activation energy of the transition states by ab initio calculation at B3LYP/6-31G* level of theory. The superscript a indicates the activation energy obtained by including solvent effects in the transition state.

asterisk in Figure 4B), suggesting that **10** was formed directly from **11k** without forming the corresponding phenylsulfoxide intermediate.

Structure Determination of the Cross-Linked Adducts. It has been shown that both the phenylsulfide and phenylsulfoxide precursors produce the 2-amino-6-vinylpurine analogue as the common reactive intermediate. We next investigated the adduct structure to confirm that the cross-linking reactions take place with the 4-amino group of the target cytidine. The ^1H NMR spectrum was measured to follow the cross-linking reaction between the ODNs (**10**, **11k**, and **12c**) and the target ODN (**13**) with cytidine at the reaction site. Reaction was performed at 30 °C in the D_2O buffer containing 0.1 M NaCl and 5 mM KH_2PO_4 at pH 5.0 by using 1.3 mM each ODNs. Figure 5A shows selected regions of the H–H COSY spectrum of the reaction between **10** and **13**, where all six correlations of H5–H6 of cytidines were observed, and is similar to that of the natural duplex (**15:13**) (Figure 5C). According to the progress of the cross-linking reaction, the signal marked “a” was decreased, and a new signal marked “b” appeared (Figure 5B). These results have suggested that the signal marked “a” is due to cytidine, and the signal marked “b” corresponds to the cross-linked cytidine. Downfield shift of H5 and H6 caused by alkylation of 4-NH₂ of cytidine accords with the results of the monomer adduct between the cytidine and the 2-amino-6-vinylpurine nucleoside derivative (Figure 6, E). Its COSY spectra showed a new signal “c” at pH 7.0 (Figure 5D) in addition to “b”. Since the signal “b” increased as pH was lowered, the signals “c” and “b” probably correspond to nonprotonated and protonated cytidine of the adduct (**14**), respectively. ^1H NMR measurements of the cross-linking reaction with **11k** and **12c** produced the same change, and have proven that the adducts from the three experiments are identical (peak **14** of Figure 4, panels A, B, and C). Attempts to isolate and determine the adduct structure by degradation of **14** were not successful, because enzymatic digestion was inhibited near the cross-linked sites. Therefore, we carried out the cross-linking reaction with the ODNs (**15a**) that contains the 2-amino-6-vinylpurine derivative

at the 5′-end and its complementary strand (**16**) (Figure 6). The corresponding cross-linked adduct (**17**) was completely hydrolyzed with SVPD (snake venom phosphodiesterase) and BAP (bacterial alkaline phosphatase) to produce the nucleosides (Figure 6C). The peak **18** was proven to be identical with the authentic alkylated adduct that was prepared from the 2′-deoxynucleoside derivatives of 2-amino-6-vinylpurine and cytidine by HPLC, ^1H NMR, and mass measurements (Figure 6D,E). The same adducts were also obtained from the cross-linking reactions with the other two ODNs (**15b** and **15c**). These results have clearly indicated that the three cross-linking agents, 2-amino-6-vinyl-, 2-amino-6-(2-phenylsulfinyl)ethyl-, and 2-amino-6-(2-*o*-carboxyphenylthio)ethylpurine derivatives, produce the same cross-linked adducts with the 4-amino group of the target cytidine.

Discussion

A Plausible Mechanism of in Situ Activation. We designed the cross-linking reaction initially based on semiempirical MO calculations (PM3) on N1-protonated 2-amino-6-vinylpurine (**1**) ($pK_a = 3.7$).⁴⁰ However, ab initio MO calculations have indicated that this process associates with high activation energy of $E_a = 53.3 \text{ kcal/mol}$ for direct proton transfer from **20** to **21** (Figure 7). Then, MO calculations were performed on an alternative mechanism with the imino tautomer of cytosine (**22**) to produce a transition state (**23**) with a lower activation energy of 20.9 kcal/mol (Figure 7). Since the imino tautomer is in equilibrium with the amino tautomer, the pathway from **22** to **24** may account for the rapid alkylation rate of the 2-amino-6-vinylpurine derivative with the target cytidine.

The in situ activation mechanism was designed so as to generate the reactive vinyl group of 2-aminopurine (**1**) from its phenylsulfoxide precursor (**3**) (Figure 1). To check this design concept, transformation of the phenylsulfoxide derivative (**12c**) was followed by HPLC and MALDI-TOF MS, and it has been proven that the ODN (**10**) was formed under the conditions of cross-linking (Figure 4D).

It is surprising that **10** is formed from **12c** in the buffer, because the corresponding monomer phenylsulfoxide (**3**)

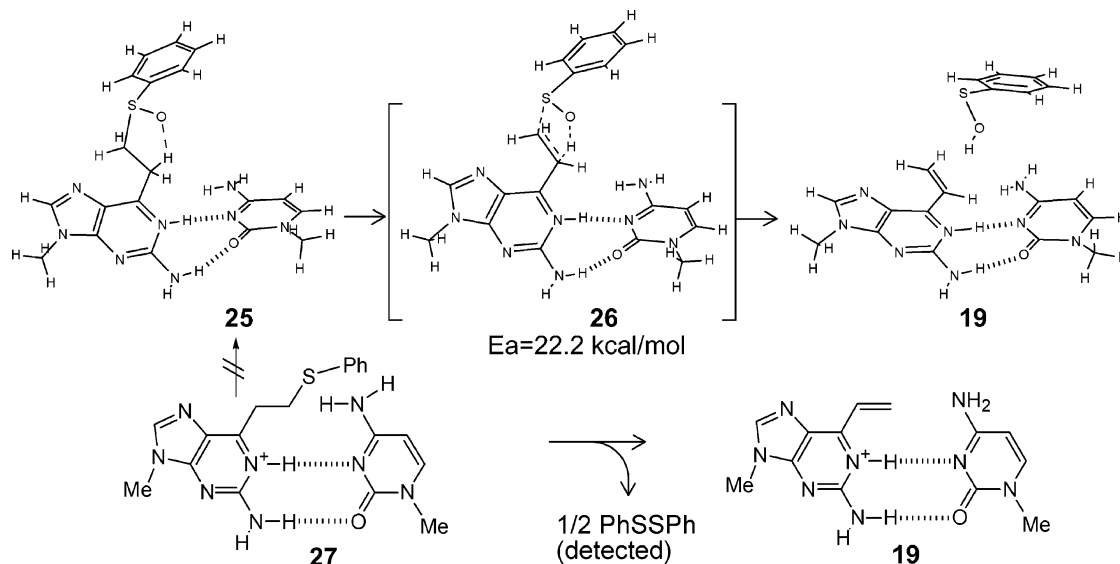


FIGURE 8. Plausible pathways of in situ activation.

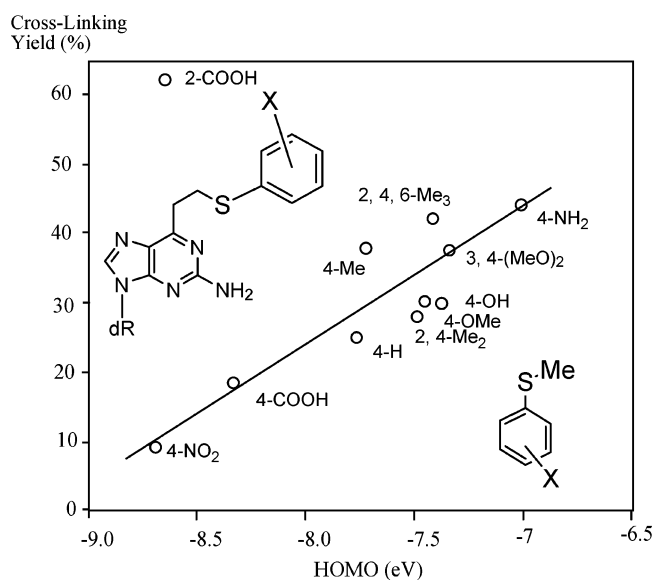


FIGURE 9. Relationship between HOMO energy of substituted thioanisole and cross-linking yield (%). Data were taken from Table 1. The HOMO ab initio calculation was performed on the substituted thioanisole at the 6-31G** level.

is very stable in the organic solvents.⁴³ It should be noted that complexation with cytosine effects to reduce the activation energy of elimination of the phenylsulfoxide from $E_a = 31.2$ kcal/mol in the monomer to $E_a = 22.2$ kcal/mol in the complex with cytosine (**25** to **19**). The experimental facts and ab initio calculations have indicated that the nature of the target-promoted activation of the phenylsulfoxide derivative is lowering the activation energy of the elimination by complexation with the target cytosine.

Detection of 2-carboxyphenyl disulfide in the cross-linking reaction with **11k** ($X = 2\text{-COOH}$) (the peak marked with an asterisk in Figure 4B) suggests the direct formation of **10** (**27** to **19**, Figure 8) not through the corresponding sulfoxide derivative (**25**). The experimental fact that the cross-linking of **11k** with the target ODN

is much faster than the formation of **10** in the nontarget duplex (Figure 4D) clearly indicates that this activation is also promoted selectively by hybridization with the target ODN. The results that 2-COOH of **11k** is more effective than 4-COOH of **11m** and that electron-donating groups give higher yields (Table 1) suggest that protonation of the sulfur atom of the phenylsulfide might accelerate elimination to the vinyl structure. However, this hypothesis was ruled out by MO calculations, because the activation energy for elimination of the phenylsulfide group was not lowered by protonation on the sulfur atom. On the other hand, when the cross-linking yields of **11** (Table 1) are plotted against the HOMO energy of substituted thioanisoles as their structural components, a linear correlation is obtained (Figure 9). Figure 9 clearly suggests that an activation process of the sulfide derivative of **11** may contain an HOMO energy-related one. The 2-COOH-substituted derivative (**11k**) produced a higher cross-linking yield than that expected from its HOMO energy, suggesting that the 2-COOH group provides additional rate enhancement effects, although its mechanism is uncertain. Further study is now ongoing to reveal the activation mechanism of the phenylsulfide precursors.

Conclusion

We have established a new target-promoted cross-linking reaction with the use of 2-amino-6-vinylpurine derivatives. The validity of the new concept has been successfully demonstrated by the fact that the stable phenylsulfide precursors are activated selectively in the target duplex to form cross-linked products with cytosine. The new cross-linking agents are characteristic in that no chemical or biological reagents are needed for the activation except for the duplex formation between the reactive ODN and the target strand. It has been concluded that the nature of the inducible reactivity of the phenylsulfoxide- and the phenylsulfide-nucleoside derivative is acceleration of their elimination to the 2-amino-6-vinylpurine through the selective processes in the duplex with the ODN having cytosine at the target site.

Although detailed mechanisms of the activation process are still uncertain, stability, selectivity, and reactivity of the new cross-linking agents will be beneficial to antisense and antigene methods, and their biological applications are now in progress.

Experimental Section

2-Amino-9-(3',5'-di-*O*-*tert*-butyldimethylsilyl-2'-deoxy-D-ribofranosyl)-6-(2-methylthioethyl)purine (5). To a solution of 2-amino-9-(3,5-di-*O*-*tert*-butyldimethylsilyl-2'-deoxy-D-ribofranosyl)-6-vinylpurine (**1**) (1.1 g, 2.2 mmol) in CH₃CN (10 mL) was added methylmercaptane sodium salt (15% in water) (1.2 mL, 2.6 mmol) at room temperature. After being stirred for 20 min, the reaction mixture was diluted with ethyl acetate (50 mL), then washed with H₂O and brine. The organic layer was dried over anhydrous Na₂SO₄, filtered, and concentrated under reduced pressure. The residue was purified by silica gel chromatography (chloroform–methanol 97:3, v/v) to afford **5** as a pale yellow oil (1.1 g, 2.03 mmol, 93%): IR (neat) 3400, 1600 cm⁻¹; ¹H NMR (CDCl₃, 400 MHz) δ 8.02 (1H, s), 6.32 (1H, t, *J* = 6.3 Hz), 5.21 (2H, br s), 4.58 (1H, dt, *J* = 5.6, 3.0 Hz), 3.99 (1H, dd, *J* = 6.9, 3.3 Hz), 3.77 (2H, m), 3.33 (2H, t, *J* = 6.6 Hz), 3.03 (2H, t, *J* = 6.6 Hz), 2.65–2.32 (2H, m), 2.18 (3H, s), 0.90 (18H, s), 0.10 (12H, s); ¹³C NMR (125 MHz, CDCl₃) δ -5.5, -5.4, -4.8, -4.7, 15.4, 18.0, 18.4, 25.7, 25.9, 32.0, 32.9, 40.6, 62.8, 72.1, 83.5, 87.6, 127.3, 139.3, 152.4, 159.5, 161.3; FABMS (*m/z*) 554 (M + 1)⁺; HRFABMS calcd for C₂₅H₄₈N₅O₃Si₂S 554.3016, found 554.3066.

2-Phenoxyacetyl amino-9-(3',5'-di-*O*-*tert*-butyldimethylsilyl-2'-deoxy-D-ribofranosyl)-6-(2-methylthioethyl)purine (6). To a solution of **5** (800 mg, 1.45 mmol) in dry CH₃CN (3.0 mL) was added 1-hydroxybenzotriazole (490 mg, 4.3 mmol) in dry pyridine solution (3.0 mL) in the presence of 4 Å molecular sieves at room temperature. After the resulting mixture was stirred for 1 h, freshly distilled phenoxyacetyl chloride (0.62 mL, 4.3 mmol) was added slowly to the reaction mixture. The reaction mixture was stirred for an additional 3 h, diluted with ethyl acetate (50 mL), and washed with H₂O and brine. The organic layer was dried over anhydrous Na₂SO₄, filtered, and concentrated under reduced pressure. The residue was purified by silica gel chromatography (hexanes–ethyl acetate 7:3, v/v) to give **6** as a pale yellow oil (747 mg, 1.09 mmol, 75%): IR (neat) 3400, 1720, 1600 cm⁻¹; ¹H NMR (CDCl₃, 400 MHz) δ 8.90 (1H, br s), 8.25 (1H, s), 7.38–7.31 (2H, m), 7.08–7.01 (3H, m), 6.47 (1H, t, *J* = 6.6 Hz), 4.79 (2H, br s), 4.64 (1H, dt, *J* = 5.6, 3.0 Hz), 4.00 (1H, dd, *J* = 7.3, 3.3 Hz), 3.88 (1H, dd, *J* = 11.2, 3.3 Hz), 3.77 (1H, dd, *J* = 11.2, 3.3 Hz), 3.44 (2H, t, *J* = 7.3 Hz), 3.07 (2H, t, *J* = 7.3 Hz), 2.73–2.44 (2H, m), 2.18 (3H, s), 0.91 (18H, s), 0.10 (12H, s); ¹³C NMR (125 MHz, CDCl₃) δ -5.5, -5.4, -4.8, -4.7, 15.4, 18.0, 18.4, 25.7, 25.9, 31.8, 32.7, 40.9, 62.8, 68.0, 72.0, 84.2, 88.0, 114.9, 122.2, 129.7, 130.5, 142.4, 151.3, 151.5, 157.1, 161.5, 166.3; FABMS (*m/z*) 688 (M + 1)⁺.

2-Phenoxyacetyl amino-9-(2'-deoxy-D-ribofranosyl)-6-(2-methylthioethyl)purine (7). To a solution of **6** (600 mg, 0.87 mmol) in dry THF solution (1.0 mL) was added *n*-Bu₄NF in THF solution (1.0 M solution, 2.62 mmol, 2.62 mL) at 0 °C. After 1 h, the reaction mixture was concentrated under reduced pressure. The residue was purified by silica gel chromatography (CHCl₃–MeOH 95:5, v/v) to give the diol **7** as a colorless crystal (392 mg, 0.85 mmol, 98%): mp 158 °C; IR (neat) 3400, 1720, 1600 cm⁻¹; ¹H NMR (*d*-DMSO, 400 MHz) δ 9.10 (1H, br s), 8.03 (1H, s), 7.38–7.31 (2H, m), 7.08–7.01 (3H, m), 6.31 (1H, t, *J* = 6.3 Hz), 5.10 (1H, m), 4.70 (2H, s), 4.15 (1H, dd, *J* = 5.6, 2.6 Hz), 3.90 (1H, m), 3.43 (2H, t, *J* = 7.3 Hz), 3.07 (2H, t, *J* = 7.3 Hz), 3.03 (1H, m), 2.41 (1H, m), 2.18 (3H, s); ¹³C NMR (125 MHz, *d*-DMSO) δ 14.4, 31.0, 31.0, 32.1, 61.6, 67.2, 70.6, 83.2, 87.9, 90.1, 99.4, 114.4, 120.8, 129.3, 143.2, 151.1, 152.0, 157.9, 160.4, 167.3; FABMS (*m/z*) 460 (M + 1)⁺. Anal. Calcd for C₂₁H₂₅N₅O₅: C, 54.89; H, 5.48; N, 15.24. Found: C, 54.66; H, 5.49; N, 15.09.

2-Phenoxyacetyl amino-9-[5'-*O*-dimethoxytrityl-3-*O*-(*N,N*-diisopropyl-2-cyanoethylphosphoramidyl)-2'-deoxy-D-ribofranosyl]-6-(2-methylthioethyl)purine (8). A solution of **7** (310 mg, 0.67 mmol) in dry pyridine (3.0 mL) was stirred for 1 h in the presence of 4 Å molecular sieves at 0 °C. Then dimethoxytrityl chloride (343 mg, 1.0 mmol) was added into the solution and the mixture was stirred for 2 h. The resulting mixture was diluted with chloroform (30 mL) and washed with saturated aqueous NaHCO₃, H₂O, and brine. The organic layer was dried over anhydrous Na₂SO₄, filtered, and concentrated under reduced pressure. The residue was purified by silica gel chromatography (chloroform–MeOH 95:5, 0.5% pyridine, v/v) to afford 2-phenoxyacetyl amino-9-(5'-*O*-dimethoxytrityl-2'-deoxy-D-ribofranosyl)-6-(2-methylthioethyl)purine as a colorless oil (500 mg, 0.61 mmol, 90%): ¹H NMR (CDCl₃, 400 MHz) δ 8.93 (1H, br s), 8.11 (1H, s), 7.68–7.00 (14H, m), 6.79–6.73 (4H, m), 6.56 (1H, t, *J* = 6.3 Hz), 4.87 (1H, dt, *J* = 5.9, 3.0 Hz), 4.68 (2H, br s), 4.17 (1H, m), 3.75 (6H, s), 3.48–3.33 (4H, m), 3.06 (2H, t, *J* = 6.9 Hz), 2.87–2.57 (2H, m), 2.18 (3H, s); FABMS (*m/z*) 761 (M)⁺.

To a solution of the above product (110 mg, 0.14 mmol) in dry dichloromethane (3.0 mL) was added diisopropylethylamine (0.15 mL, 0.86 mmol) at 0 °C in the presence of 4 Å molecular sieves. After the resulting mixture was stirred for 30 min, 2-cyanoethyl *N,N*-diisopropylchlorophosphoramidite (0.11 mL, 0.43 mmol) was added. The reaction mixture was stirred for an additional 30 min at the same temperature. The resulting mixture was diluted with ethyl acetate (30 mL) and washed with saturated aqueous NH₄Cl, H₂O, and brine. The organic layer was dried over anhydrous Na₂SO₄, filtered, and concentrated under reduced pressure. The residue was purified by silica gel chromatography (hexanes–ethyl acetate 1:1, v/v) to afford **8** as a colorless oil (123 mg, 0.13 mmol, 93%): ¹H NMR (CDCl₃, 400 MHz) δ 8.81 (1H, br s), 8.14 (1H, s), 7.39–7.01 (14H, m), 6.76 (4H, dd, *J* = 6.8, 2.0 Hz), 6.47 (1H, t, *J* = 6.3 Hz), 4.78 (3H, m), 4.29 (1H, m), 3.88–3.78 (2H, m), 3.76 (6H, s), 3.74–3.56 (4H, m), 3.47–3.32 (2H, m), 3.37 (2H, t, *J* = 6.3 Hz), 2.88–2.60 (2H, m), 2.64 (2H, t, *J* = 6.3 Hz), 2.18 (3H, s), 1.19 (6H, d, *J* = 6.9 Hz), 1.17 (6H, d, *J* = 6.9 Hz); ³¹P NMR (CDCl₃, 162 MHz) δ 148.8; FABMS (*m/z*) 962 (M)⁺.

Oligonucleotide Synthesis. All oligonucleotides were synthesized at a 1 μmol scale on Cyclon Plus DNA-synthesizer (Milligen/Bioscience) with standard β-cyanoethyl phosphoramidite chemistry. The 5'-terminal dimethoxytrityl-bearing ODNs were removed from the solid support by treatment with 0.1 M NaOH (2.0 mL) and the solution was neutralized with CH₃COOH instantly. The crude product was purified by reverse-phase HPLC with C-18 column (nacalai tesque: COSMOSIL 5C18-AR-II, 10 × 250 mm) by a linear gradient of 10–40%/20 min of acetonitrile in 0.1 M TEA buffer at a flow rate of 4 mL/min. The dimethoxytrityl group of the purified ODN was cleaved with 10% AcOH and the mixture was additionally purified by HPLC with the same elution method. MALDI-TOF MS (*m/z*) **9**: calcd 4812.83, found 4809.78

Preparation of the ODN 10. To a solution of ODN **9** (0.97 μmol, 1 mL) was added a solution of magnesium monopropylphthalate (MMPP) (2.9 μmol) in carbonate buffer (50 μL) adjusted to pH 10 at room temperature. After 30 min, NaOH (4 mol/L, 150 μL) was added, and the mixture was left for an additional 30 min. The resulting mixture was dialyzed with a buffer (0.1 M NaCl, 5 mM potassium phosphate, pH 7.0) to give ODN (**9**) (0.75 μmol). MALDI-TOF MS (*m/z*) **10**: calcd 4764.83, found 4762.97.

Preparation of the ODN 11a–l. To a solution of ODN **10** (0.41 μmol, 1.0 mL) was added a solution of substituted thiophenol in CH₃CN (2.1 μmol, 20 μL) at room temperature. After 30 min, the resulting mixture was purified by HPLC to give ODN **11a–l**. The yields and MALDI-TOF MS (*m/z*) data of **11a–l** are summarized in Table 2.

Preparation of the ODN 12a–g,k. To a solution of ODN **11** (0.97 μmol, 1 mL) was added a solution of magnesium monopropylphthalate (MMPP) (2.9 μmol) in carbonate buffer (50

TABLE 2.

ODNs	yield (%)	MALD-TOF MS	
		caclcd	found
11a	38	4919.8	4919.1
11b	62	4952.7	4951.9
11c	60	4874.8	4874.6
11d	53	4904.8	4903.8
11e	63	4890.8	4891.8
11f	57	4888.8	4888.8
11g	57	4889.0	4886.7
11h	55	4902.9	4900.3
11i	47	4934.9	4934.9
11j	42	4916.9	4919.8
11k	55	4918.8	4919.2
11l	50	4918.8	4915.7
12a		4935.8	4933.4
12b		4968.7	4967.3
12c		4890.8	4888.9
12d		4920.8	4917.7
12e		4906.8	4907.8
12f		4904.8	4906.3
12g		4905.0	4902.5
12k		4934.8	4936.7

μL) adjusted to pH 10 at room temperature. After 30 min, the reaction mixture was dialyzed with a buffer (0.1 M NaCl, 5 mM potassium phosphate, pH 7.0) to give ODN (**12**) (0.75 μmol), and was used without further purification. The MALDI-TOF MS (m/z) data of **12a–g,k** are summarized in Table 2.

Electrophoresis Assay of the Cross-Linking Reaction.

The complementary ODN was 5'-end-labeled by treatment with T4 polynucleotide kinase and [γ - ^{32}P] ATP under standard conditions. The reaction was performed with 7 μM of the sulfide ODN, 3 μM of the complementary unlabeled ODN, and labeled ODN (1×10^4 cpm) as a tracer in a buffer of 100 mM NaCl and 50 mM MES buffer at pH 5.0. The reaction mixture was incubated at 37 °C for 24 h. The reaction was stopped by the addition of the loading dye (95% formamide, 20 mM EDTA, 0.05% xylene cyanol, and 0.05% bromophenol blue) and heating at 90 °C for 10 min. The cross-linked products were analyzed by a denaturing 20% polyacrylamide gel electrophoresis containing urea (7 M) with TBE buffer at 300 V for 1.5 h. The labeled bands were visualized by autoradiography and quantified with use of a BAS 2500 Phosphor Imager.

Isolation of the Cross-Linking Adducts. The cross-linking reaction was performed with the reactive ODN (0.3 mM) and the complementary ODN (0.3 mM) in a buffer (100 mM NaCl, 50 mM MES buffer, pH 5.0) at 30 °C. The total volume of the reaction mixture was 1.5 mL. After 24 h, the cross-linking adduct was purified by HPLC with an ODS column (nacalai tesque: COSMOSIL 5C18-AR-II, 10×250 mm), using a linear gradient of 5–30%/20 min acetonitrile in 50 mM ammonium acetate.

NMR Measurements. NMR samples were lyophilized from 99.96% D_2O and dissolved in 300 μL of the buffer containing 0.1 M NaCl, 5 mM KH_2PO_4 at pH 7.0 in D_2O . The total concentration of the duplex was 1.3 mM. ^1H NMR spectra were recorded on a Varian Inova 600 spectrometer at 600 MHz. The 1D spectra were 65536 complex points with 64 scan averaged. The 2D-DQF COSY spectra were recorded at 30 °C with sweep widths of 6492.5 Hz in both dimensions, and consisted of 2048 data points in t_2 and 512 increments in t_1 . The residual HDO peak was suppressed by presaturation.

Molecular Orbital Calculations. Ab initio MO calculations were performed by using the GAUSSIAN94 program to optimize stable and transition state (TS) structure at the B3LYP/6-31G* level of theory for Figure 7. Vibrational frequency calculations showed all the transition states to have only one imaginary frequency. HOMO energies of the substituted thioanisoles were calculated at the RHF/6-31G* level of theory.

Acknowledgment. This work has been supported by a Grant-in-Aid for Scientific Research (B) and (C) from Japan Society for the Promotion of Science (JSPS) and Priority Area (A)(2) (Molecular Synchronization) from the Ministry of Education, Culture, Sports, Science and Technology (MEXT), CREST from the Japan Science and Technology Agency (JST), Kyushu University P&P “Green Chemistry” Program, and the Research Consortium from Kyushu Bureau of Economy, Trade and Industry.

Supporting Information Available: Experimental details and ^1H , ^{13}C , and ^{31}P NMR spectra of nucleoside analogues in Scheme 2. This material is available free of charge via the Internet at <http://pubs.acs.org>.

JO048298P